

See discussions, stats, and author profiles for this publication at: <https://www.researchgate.net/publication/248395575>

Application of Time-Dependent Density Functional Theory and Optical Spectroscopy toward the Rational Design of Novel 3,4,5-Triaryl-1-R-1,2-diphospholes

ARTICLE *in* THE JOURNAL OF PHYSICAL CHEMISTRY A · JULY 2013

Impact Factor: 2.69 · DOI: 10.1021/jp4043914 · Source: PubMed

CITATIONS

4

READS

45

7 AUTHORS, INCLUDING:



Elena E. Zvereva

Russian Academy of Sciences

37 PUBLICATIONS 606 CITATIONS

SEE PROFILE



Stefan Grimme

University of Bonn

475 PUBLICATIONS 31,151 CITATIONS

SEE PROFILE



Sergey A Katsyuba

Russian Academy of Sciences

105 PUBLICATIONS 881 CITATIONS

SEE PROFILE



Almaz Zagidullin

Russian Academy of Sciences

17 PUBLICATIONS 68 CITATIONS

SEE PROFILE

Application of Time-Dependent Density Functional Theory and Optical Spectroscopy toward the Rational Design of Novel 3,4,5-Triaryl-1-R-1,2-diphospholes

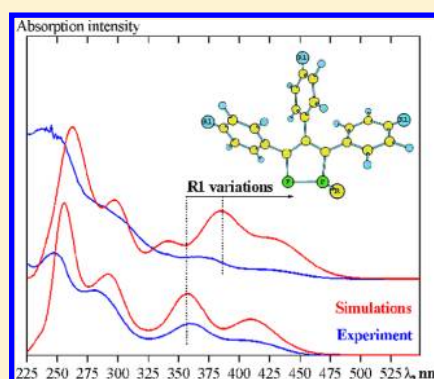
Elena E. Zvereva,^{*,†,‡} Stefan Grimme,^{*,‡} Sergey A. Katsyuba,[†] Timur I. Burganov,[†] Almaz A. Zagidullin,[†] Vasily A. Milyukov,[†] and Oleg G. Sinyashin[†]

[†]A.E. Arbuzov Institute of Organic and Physical Chemistry, Kazan Scientific Centre, Russian Academy of Sciences, Arbuzov str. 8, 420088 Kazan, Russia

[‡]Mulliken Center for Theoretical Chemistry, Institut für Physikalische und Theoretische Chemie, Universität Bonn, Beringstr. 4, 53115 Bonn, Germany

S Supporting Information

ABSTRACT: Twenty 3,4,5-triaryl-1-R-1,2-diphospholes were studied within the framework of density functional theory (DFT) and experimentally by UV/vis spectroscopy to check their suitability for opto-electronic applications. Time-dependent DFT (TD-DFT) calculations employing the PBE0 hybrid density functional combined with moderately sized def-TZVP basis set were shown to excellently reproduce the experimental absorption spectra of various 1,2-diphospholes. Frontier molecular orbital analysis reveals that HOMO and LUMO are mainly localized on the diphosphole ring and, to some extent, on the aryl moieties. The HOMO–LUMO energy gap can be easily tuned by variation of substituents introduced in para-positions of the aryl moieties and, to a lesser extent, by modification of the R group at phosphorus atom. As a result, both position and intensity of the absorption bands with highest wavelength are strongly influenced by the above structural changes. The UV-spectra simulations reveal that the introduction of donor groups like *para*-OMe, *para*-NMe₂, and *para*-N(H)Ph, which are in $n-\pi$ conjugation with the aryl moieties, should result in absorption of visible light by the corresponding 1,2-diphospholes, thus making them promising candidates for new functional materials.



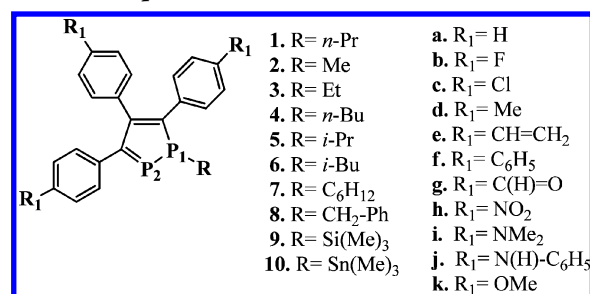
INTRODUCTION

Since the 1990s the π -conjugated materials based on organophosphorus compounds represent a valuable addition to the pool of building blocks for molecular electronics.^{1–3} Phospholes (five-membered 6π -systems with one or more phosphorus atoms) as subunits for the π -conjugated systems are the most widely investigated P-heterocycles, because they display interesting electronic properties with both high electron-accepting and electron-transporting abilities.^{4,5} The key property of these P-rings for molecular engineering of π -conjugated systems is based on their electronic structure⁶ with a reactive phosphorus center. Low aromatic character of these P-heterocycles with a low-lying LUMO, $\sigma^*(\text{P-R})-\pi^*(1,3\text{-diene})$ hyperconjugation^{7,8} and high electronic affinity allow tuning the photophysical properties of phosphole-based π -conjugated systems by chemical modifications of the reactive P-atoms and influencing the extent of conjugation over the diene moiety.^{2,8,9} Richness and diversity of phosphorus chemistry together with mentioned specific properties of organophosphorus derivatives should be fully exploited for the engineering of a wide range of novel conjugated materials.¹⁰

The main objective of this work is to rationalize the structure–property relationship of some 3,4,5-triaryl-1-R-1,2-

diphospholes (Chart 1). They are based on a five-membered ring with two neighboring phosphorus atoms, unlike the monophospholes with only one phosphorus atom in the cycle, which are the most studied and described in literature. These 1,2-diphospholes combine the structural elements of both 1H- and 2H-phospholes in one molecule, which increases its

Chart 1. 3,4,5-Triaryl-1-R-1,2-diphospholes Investigated in the Present Paper



Received: May 3, 2013

Revised: July 10, 2013

Published: July 10, 2013

aromaticity^{11–13} and, hence, most probably can change dramatically their optical properties. In present paper we study the UV/vis spectra of the title compounds and use quantum chemical calculations to better understand the origin of the absorption bands and to find their relationship with the electronic and geometrical structure of the molecules. We demonstrate that the computations can be used as a practical tool for prediction of the spectra of yet nonsynthesized molecules, thus allowing the design of new compounds performing light-absorption/emission properties necessary for promising candidates for new materials.^{1,5}

■ COMPUTATIONAL DETAILS

All calculations were performed with the Turbomole 6.4 program package.¹⁴ In the ground state SCF calculations with hybrid density functionals, the RI-JK approach for the two-electron integrals^{15–18} was employed. In general the def-TZVP¹⁹ AO basis set with accompanying auxiliary basis sets^{20–22} was used, but the def-SVP¹⁹ and the def-QZVP¹⁹ AO basis sets were tested as well. All structures were optimized with the PBE functional.^{23,24} Time-dependent density functional response theory (TD-DFT)^{25,26,16,27} has been employed to compute the vertical excitation energy (i.e., absorption wavelength) and oscillator strength for the ground state optimized geometries in the gas phase. The influence of surrounding media was neglected, as inclusion of weakly interacting solvent molecules within PCM or COSMO continuum solvation models just induces a small (4–10 nm) bathochromic shift of the entire spectrum.^{28,29} Various functionals have been used in the literature for the computation of absorption spectra of organic molecules.^{28–33} The semilocal PBE²³ functional and two hybrid functionals PBE0³⁴ and B3LYP^{35,36} have been tested by comparing results of the computations with available experimental results. PBE0 and B3LYP importantly differ by the amount of nonlocal Fock-exchange included in the functional (25% vs 50%) which is known to influence excitation energies and excited state properties rather strongly.³⁰ In most cases, the spectra were broadened by Gaussian functions with a half-width at 1/e height of 0.4 eV. No energy shift has been applied. The dipole length representation is used to calculate oscillator strengths discussed in the present paper. Molecular orbitals based on PBE/def-TZVP optimized structures recalculated within Gaussian 03³⁷ (PBE0/def-TZVP) were visualized in the ChemCraft 1.6 program³⁸ with a 0.03 contour value. The diagrams were created with using Xmgrace.³⁹

■ EXPERIMENTAL SECTION

1,2-Diphospholes **1a**, **1b**, **1c**, **10a**, and **5k** were synthesized according to the earlier described protocol.⁴⁰

UV/vis spectra were recorded at room temperature on a Perkin-Elmer Lambda 35 spectrometer, using 10 mm quartz cells. Spectra were registered with a scan speed of 480 nm/min, using a spectral width of 1 nm. All samples were prepared as solutions in hexane with the concentrations of ca. $\sim 10^{-4}$ mol/L.

■ RESULTS AND DISCUSSION

Electronic Absorption Spectra in the Gas Phase from TD-DFT Calculations. Several publications were devoted to TD-DFT computations of UV/vis spectra of some monophosphole derivatives with various functional and basis

sets.^{4,8,41} No simulations of UV/vis spectra of the polyphospholes were reported, though DFT and MP2 quantum chemical methods have been applied for the analysis of structure, IR spectra and magnetic properties of polyphospholes.^{13,42}

Therefore, it was first necessary to find an acceptable level for the computations yielding within reasonable CPU times reliable results. For this purpose the UV/vis spectrum of **1a** was recorded and used as a benchmark (Figure 1) for the simulations. The experimental spectrum comprises an intensive band at 211 nm and a weaker band at 244 nm due to absorptions of aromatic units^{43,44} and three even weaker bands at 281, 359, and 408 nm, which preliminarily can be attributed with absorptions of 1,2-diphosphole moiety. It should be noted

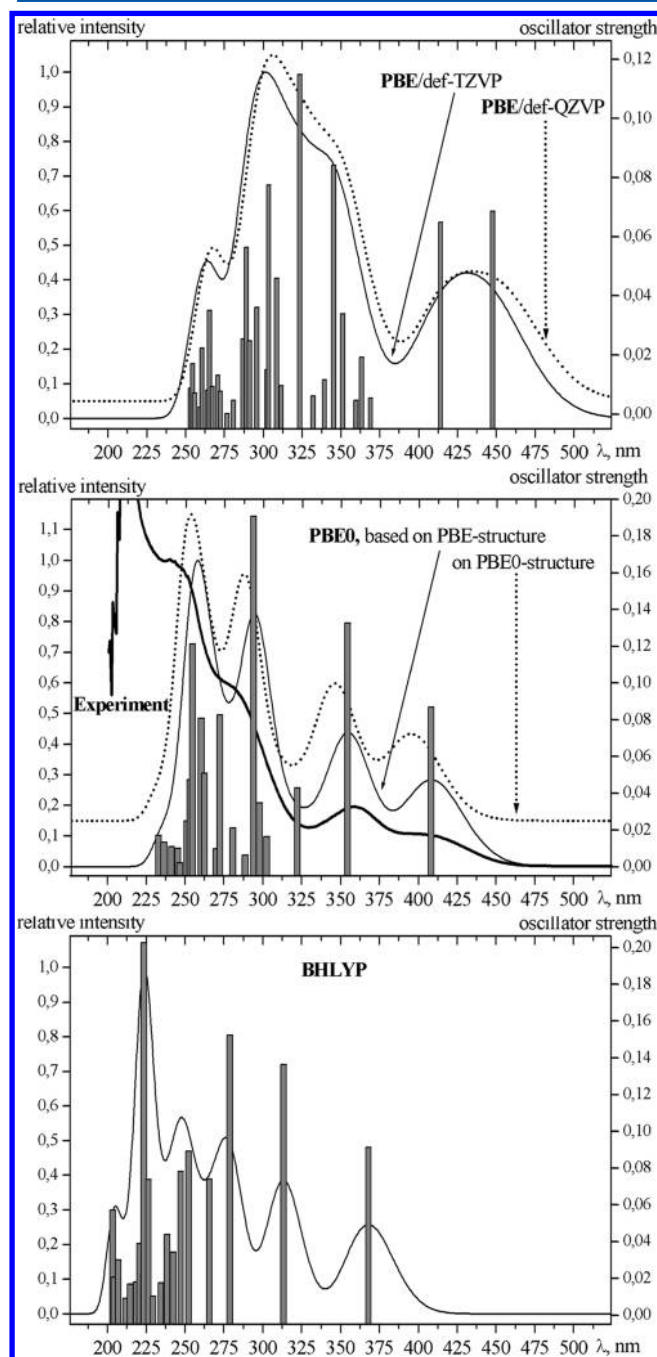


Figure 1. Experimental (bold) and simulated UV/vis absorption spectra of **1a** (calculated with different functionals and basis sets).

that the lowest excitation at 408 nm is bathochromically shifted relative to the positions of the HOMO \rightarrow LUMO transitions in 1,2,5-triphenyl- and pentaphenyl-phospholes.^{1,45}

To interpret the observed absorption bands, quantum chemical calculations were conducted. First, the structure of **1a** was optimized at the PBE/def-TZVP level. The spectrum from the 30 lowest singlet states calculated for the optimized ground state structure is in reasonable agreement with the experimental spectrum (Figure 1). Test calculations with the extended def-QZVP AO basis set took considerably more CPU-time but did not lead to any noticeable changes in the simulated spectrum.

As hybrid functionals are expected to produce better quality simulations,^{28,30} the spectrum was recalculated (Figure 1) with the hybrid functionals PBE0²³ (25% of Fock exchange) and B3LYP³⁵ (50% of Fock exchange) for structure **1a** optimized at the same levels of theory. In these cases only 20 singlet states were computed because the use of hybrid functionals substantially increased the computational time in comparison to the case of PBE. Moreover, hybrid functional produces less artificial so-called “ghost” states due to the self-interaction error^{46–48} in the semilocal part of the functional, and hence, for the same spectral energy range a smaller number of states is required.

The PBE0 functional was reported to yield accurate simulations of absorption spectra of benzosiloles,²⁹ while the B3LYP functional was successfully applied earlier for UV/vis and CD spectra simulation of some monophosphole derivatives.⁴⁹ Nevertheless, the UV/vis spectrum of **1a** obtained with the B3LYP functional (Figure 1) agrees less well with the experimental spectrum than for PBE0. In fact the PBE0 functional with a smaller contribution of Fock exchange yields an excellent agreement with the experimental spectrum in the region 475–225 nm, both in band positions as well as their relative intensities (absolute intensities were computed but are experimentally not available for comparison). Thus, only the PBE0 functional was further considered for the spectra simulations.

As the calculations with the use of hybrid functionals are rather CPU-time-consuming, some simplifications are highly desirable. We reduced the necessary computational time considerably using the resolution-of-identity (RI) approximation.¹⁵ The spectra simulated with and without RI-approximation completely coincided with each other. Further minimization of the computational expense was achieved by a PBE0 simulation performed for the structure of **1a** optimized with the computationally more efficient PBE functional. The spectrum obtained in this way is practically identical to that from the structure directly optimized within the same hybrid functional, except for a small bathochromic shift of all bands by ~ 13 nm (Figure 1). This effect can be traced back to systematically smaller bond lengths (by about 1–2 pm) in the PBE0 compared to the PBE treatment. Thus, for the studied 1,2-diphospholes it is acceptable to calculate the spectra at the PBE0/def-TZVP level of theory (for 20 singlet states) on PBE/def-TZVP optimized structures. In the case of limited computational resources the smaller def-SVP AO basis set can be used as well, because together with the PBE0 functional it also provides UV spectra in good agreement with the experimental ones (see Figure S1, ESI). Finally, it was established that variation of conformation of the alkyl substituent at the P1 atom does not introduce pronounced changes to the calculated spectra; therefore, there is no

necessity for time-consuming searches of the dominant conformers (Figure S2, ESI). In the following only data obtained within the above simplified approach are discussed.

The excitation energies and oscillator strengths of all 20 calculated transitions are listed in Table 1. According to the

Table 1. Experimental UV/vis Absorption Bands and TD-DFT (PBE0/def-TZVP) Calculated Excitation Energies (nm), Oscillator Strengths (f), and Assignments of the Electronic Transitions (N) of Molecule **1a^a**

N	energy/f	assignment	λ_{abs}
1	408/0.087	98 \rightarrow 99 (94.6%)	409
2	354/0.133	97 \rightarrow 99 (92.8%)	358
3	322/0.043	96 \rightarrow 99 (93.6%)	
4	302/0.017	94 \rightarrow 99 (57.2%)	
		93 \rightarrow 99 (20.2%)	
		98 \rightarrow 100 (11.9%)	
5	298/0.035	95 \rightarrow 99 (61.1%)	
		98 \rightarrow 100 (24.9%)	
6	294/0.191	98 \rightarrow 100 (52.6%)	279
		95 \rightarrow 99 (29.6%)	
7	289/0.006	93 \rightarrow 99 (48.8%)	
		94 \rightarrow 99 (29.6%)	
8	281/0.021	92 \rightarrow 99 (54.1%)	
		98 \rightarrow 101 (23.1%)	
		93 \rightarrow 99 (13.2%)	
9	272/0.083	98 \rightarrow 102 (83.4%)	
10	270/0.009	98 \rightarrow 101 (66.0%)	
		92 \rightarrow 99 (19.1%)	
11	262/0.051	97 \rightarrow 100 (43.5%)	
		91 \rightarrow 99 (35.8%)	
12	260/0.081	97 \rightarrow 100 (47.8%)	
		91 \rightarrow 99 (24.9%)	
		98 \rightarrow 103 (9.9%)	
13	255/0.121	98 \rightarrow 103 (61.8%)	242
		90 \rightarrow 99 (16.3%)	
14	253/0.047	90 \rightarrow 99 (58.9%)	
		91 \rightarrow 99 (10.1%)	
15	251/0.025	98 \rightarrow 104 (48.7%)	
		98 \rightarrow 105 (12.7%)	
16	247/0.002	98 \rightarrow 105 (43.0%)	
		98 \rightarrow 104 (22.6%)	
17	245/0.010	97 \rightarrow 101 (38.3%)	
		98 \rightarrow 105 (22.4%)	
18	241/0.011	97 \rightarrow 102 (72.5%)	
		97 \rightarrow 101 (18.4%)	
19	236/0.013	96 \rightarrow 100 (79.8%)	
20	233/0.017	97 \rightarrow 103 (17.7%)	
		97 \rightarrow 101 (15.1%)	
		96 \rightarrow 100 (10.6%)	

^aOnly single excitation contributions of more than 10% are given.

TD-DFT calculations the band at 408 nm in the simulated spectrum is assigned to the transition from the highest occupied molecular orbital (HOMO) to the lowest unoccupied molecular orbital (LUMO). Several frontier molecular orbitals (FMOs) of diphosphole **1a** are given in Figure 2. As can be seen, the HOMO is predominantly localized in the P=C and C=C bonds of the diphosphole-ring and partly in the aromatic substituents. The LUMO involves mainly a remaining part of the ring, including the lone pair of phosphorus atom P1. The second calculated singlet state at 354 nm is due to the HOMO-

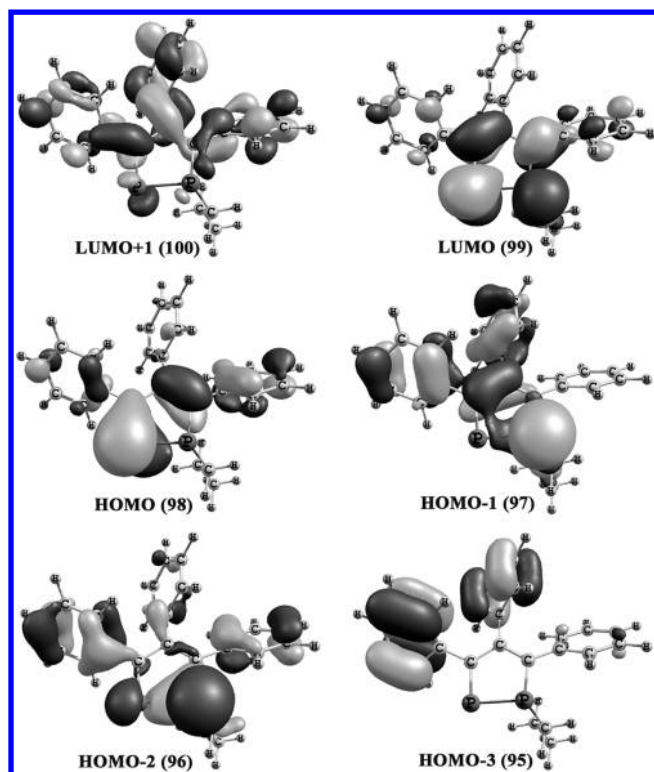


Figure 2. Some frontier molecular orbitals of **1a** and their numbers (in parentheses).

1 \rightarrow LUMO transition (92.8%). The HOMO-1 is localized in the π -system of dienic moiety and exocyclic P–C σ -bond, forming hyperconjugation and involves also the lone pair of the phosphorus atom P1 and two phenyl rings. The third relatively broad band with a maximum at 294 nm in the spectrum of **1a** is composed of four transitions, the main contributions coming from HOMO \rightarrow LUMO+1 (52.6%) and HOMO-3 \rightarrow LUMO (29.6%) excitations. Finally, the fourth band in the spectrum with a maximum at 257 nm is composed of many transitions and is difficult for straightforward interpretation.

The above assignments and composition of FMOs suggest that chemical modification of substituents both at the P1 atom and at carbon atoms of the ring should change the optical properties of the 1,2-diphospholes. Earlier it was reported that the HOMO–LUMO gap and observed absorptions of 1-R-2,5-diaryl-monophospholes depend strongly on the nature of both the R-group and aryl substituents of the monophosphole ring.^{1,9,10} A comparison of the simulated absorption spectra of model molecules **2a**–**10a** (Chart 1) demonstrates that variation of the alkyl moiety at P1 (**2a**–**7a**) does not change the HOMO \rightarrow LUMO and HOMO-1 \rightarrow LUMO energy gaps significantly (Table 2). Introduction of a benzyl substituent (**8a**) leads only to a small bathochromic shift of the first two excitations.

Introduction of $-\text{Si}(\text{CH}_3)_3$ (**9a**) or $-\text{Sn}(\text{CH}_3)_3$ (**10a**) moieties at P1 of the 1,2-diphosphole cycle increases the energy gaps between the HOMO \rightarrow LUMO and HOMO-1 \rightarrow LUMO by 0.21 and 0.12 eV, respectively, compared to **1a** (Table 2). In full agreement with the computations, the band attributed to the mentioned excitations in an experimental spectrum of **10a** (Figure 3) exhibits a hypsochromic shift relative to the position of the corresponding band in the UV spectrum of **1a**. The excellent overall agreement of the simulated spectrum of **10a** with the experimental one

Table 2. TD-DFT (PBE0/def-TZVP) Calculated Lowest Singlet Excitation Energies in the Investigated Molecules

	energies, eV (nm)	
	HOMO \rightarrow LUMO	HOMO-1 \rightarrow LUMO
1a	3.04 (408)	3.49 (354)
2a	3.03 (409)	3.51 (353)
3a	3.03 (409)	3.49 (354)
4a	3.03 (410)	3.49 (355)
5a	3.02 (411)	3.47 (357)
6a	3.09 (401)	3.51 (353)
7a	3.06 (405)	3.49 (354)
8a	2.96 (418)	3.35 (370)
9a	3.26 (380)	3.61 (343)
10a	3.25 (381)	3.61 (343)
1b	3.02 (410)	3.47 (358)
1c	3.00 (413)	3.42 (362)
1d	2.98 (415)	3.42 (363)
1e	2.90 (427)	3.24 (381)
1f	2.85 (435)	3.16 (392)
1i	2.88 (430)	3.23 (384)
1j	2.66 (465)	2.86 (433)
1k	2.66 (466)	2.80 (442)

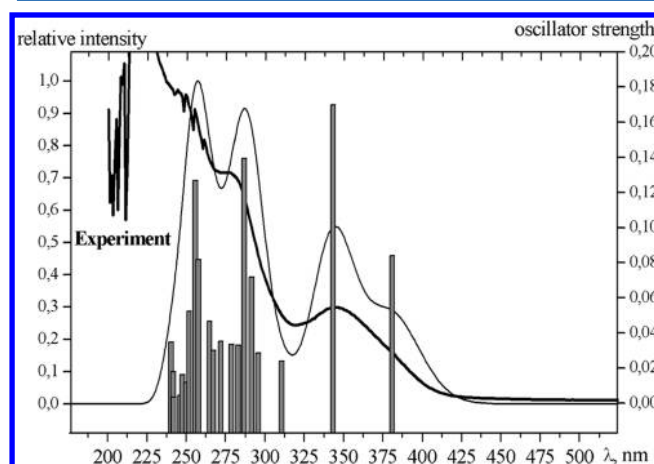


Figure 3. Experimental (bold) and simulated absorption spectra of **10a**.

demonstrates the reliability of our computational approach for the current purpose.

According to the simulations presented in the Table 2, introduction of F, Cl, or Me substituents in the para-positions of the phenyl groups causes almost negligible bathochromic shifts of the HOMO \rightarrow LUMO and HOMO-1 \rightarrow LUMO transitions of molecules **1b**–**1d** compared to **1a**. Probably, the influence of these substituents is restricted to the π -systems of the phenyl groups, but not to the diphosphole ring. These observations are supported by experimental UV/vis spectra of the *para*-F and *para*-Cl derivatives (**1b**, **1c**), which are very similar to the spectrum of **1a** and agree well with the corresponding simulated spectra (Figure S3 and S4, ESI).

Insertion of substituents $-\text{CH}=\text{CH}_2$ (**1e**) or $-\text{C}_6\text{H}_5$ (**1f**) which are able to be in conjugation with aromatic rings leads to the appearance of additional strong absorptions near 330–340 nm due to substantial shift of bands belonging to the aromatic moieties (Figure 4), similar to the earlier reported case of the *para*-substituted phenols.⁵⁰ Moreover, only a moderate bathochromic shift of two lowest transitions attributed to 1,2-

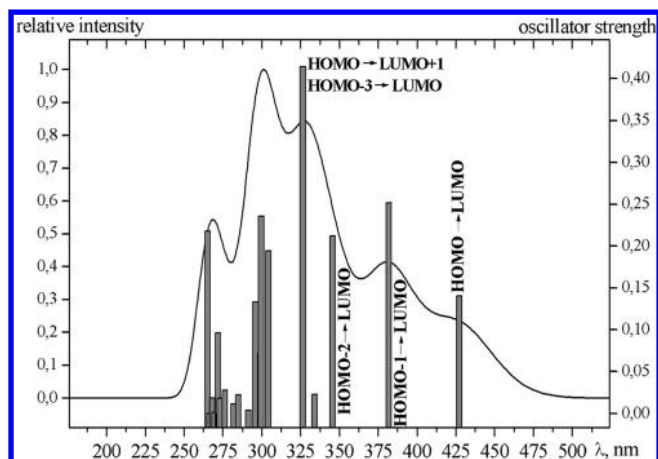


Figure 4. Simulated UV/vis absorption spectrum of **1f**.

diphosphole unit ($\text{HOMO} \rightarrow \text{LUMO}$ and $\text{HOMO-1} \rightarrow \text{LUMO}$) is calculated (Table 2).

More pronounced changes in the simulated spectra are caused by introduction of *para*-C(H)O (**1g**) and *para*-NO₂ groups (**1h**) (see Figure S, assignments are listed in the Table S2 and S3, ESI). According to the calculations in the Vis-region (>400 nm) a band at ~420 nm appears due to the $\text{HOMO} \rightarrow \text{LUMO}$ transition, whereas the $\text{HOMO-1} \rightarrow \text{LUMO}$ excitation is bathochromic shifted, and mixes with $\text{HOMO} \rightarrow \text{LUMO+1}$ and $\text{HOMO} \rightarrow \text{LUMO+2}$ transitions. As a result, the calculations yield two strong overlapping absorption bands in

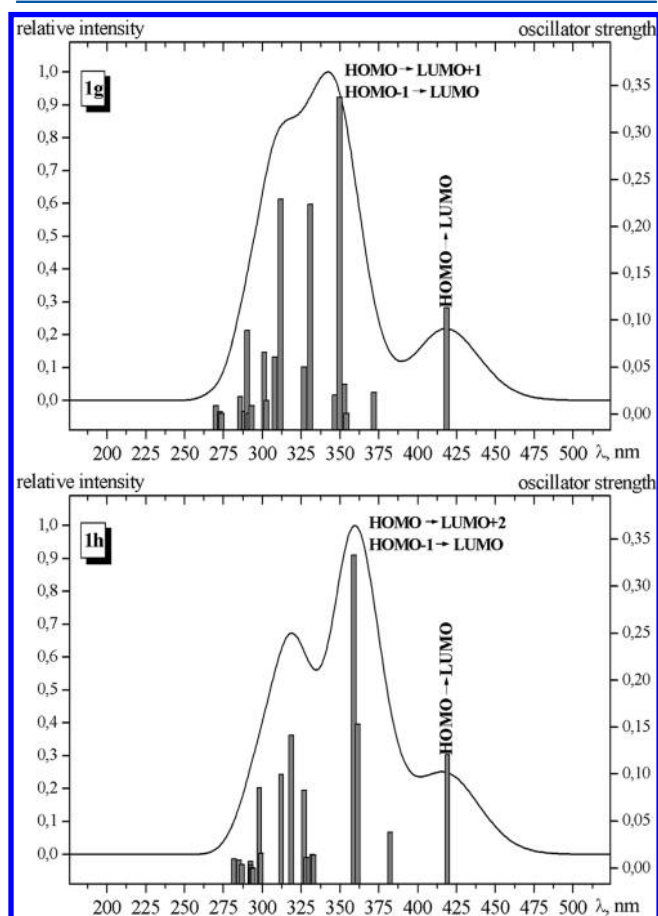


Figure 5. Simulated UV/vis absorption spectra of **1g** and **1h**.

the UV region 300–370 nm. As in the case of **1a** the HOMO of these derivatives (Figure 6) is predominantly localized in the

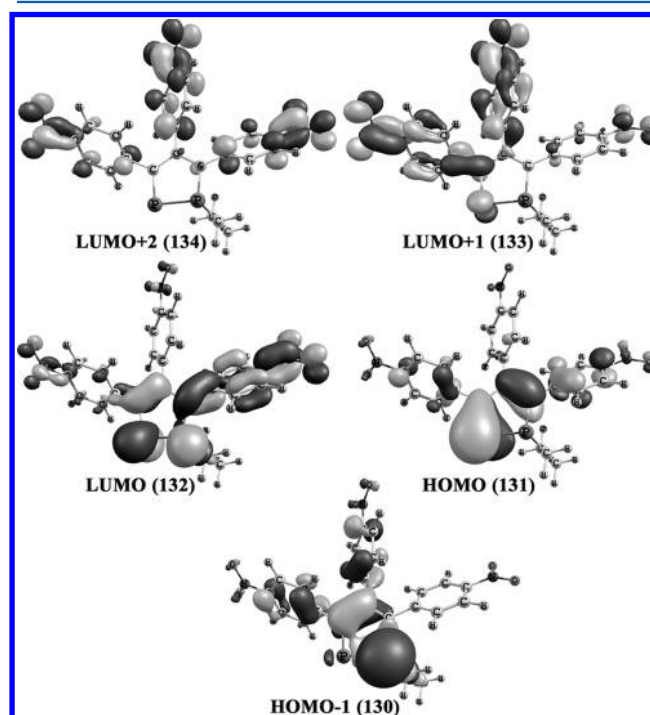


Figure 6. Some frontier molecular orbitals of **1h** (the number of the orbital is shown in the parentheses).

$\text{P}=\text{C}$ and $\text{C}=\text{C}$ bonds of the diphosphole-ring and partly in the aromatic substituents with small additions from the NO₂ group. The LUMO involves the diphosphole ring and the lone pair of phosphorus atom P1 as in the case of **1a**, but a substantial contribution from phenyl and NO₂ moieties results in moderately diminished energy gap. The main contributions to these transitions are from frontier unoccupied MOs in the aryl-substituents conjugated with electron acceptor groups (see Figure 6).

In the case of *para*-substitutions with electron-donor groups like -NMe₂ (**1i**), -N(H)Ph (**1j**), and -OMe (**1k**), the calculations show substantial changes of the energy gaps between FMOs. A similar reduction of the HOMO–LUMO energy gap due to insertion of -OMe and -N(H)Me groups was reported earlier for phosphole-based oligomers.⁵¹ As a result, three overlapped bands in the near UV/vis region appear due to transitions between $\text{HOMO} \rightarrow \text{LUMO}$, $\text{HOMO-1} \rightarrow \text{LUMO}$, and $\text{HOMO-2} \rightarrow \text{LUMO}$ orbitals, which are placed separately from another short-wavelength absorption bands (Figure 7, Table 3). The presence of electron-donor groups influences the π -systems of the phenyl moieties, but it also changes the composition of the FMOs. For these derivatives the HOMO is localized in the aromatic substituents with contribution from lone pairs of O or N atoms (Figure 8) and to a less extent at the $\text{P}=\text{C}$ and $\text{C}=\text{C}$ bonds of the diphosphole ring contrary to the HOMO of **1a** (Figure 2). The HOMO-1 is mainly spread on the two phenyl rings and lone pairs of O or N atoms, but contributions from the π -system of diene moiety, exocyclic $\text{P}-\text{C}$ σ -bond and the lone pair of phosphorus atom P1 are diminished relative to **1a**. Also as can be seen from Figure 8 for these derivatives hyperconjugation between the π -system of dienic moiety and the exocyclic $\text{P}-\text{C}$ σ -bond is

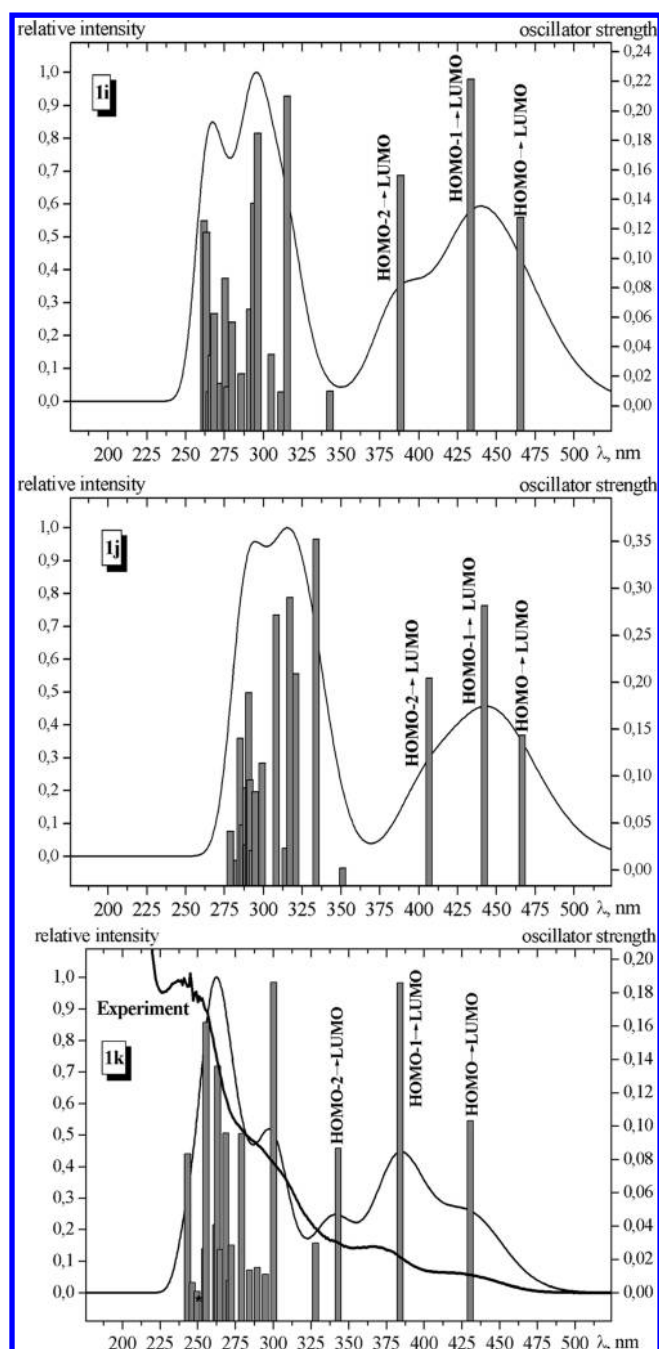


Figure 7. Simulated UV/vis absorption spectra of **1i**, **1j**, and **1k** and experimental (bold) UV/vis absorption spectrum of **5k**.

decreased dramatically and that changes the HOMO-1 composition. The HOMO-2 is formed by equal fractions from the phenyl rings, cyclic bonds and lone pairs of P1 and O and N atoms.

To validate the above predictions a derivative containing *para*-OMe substituents at the phenyl groups (**5k**) was synthesized after the TD-DFT computations had been performed according to the previously described protocol.⁴⁰ The experimental UV/vis absorption spectrum of this derivative corresponds well to the simulated spectrum of **1k** (Figure 7) and demonstrates a bathochromic shift of the first transitions in full agreement with the computational predictions (Table 3). These results clearly indicate that the $-\text{OMe}$, $-\text{N}(\text{Me})_2$, and $-\text{N}(\text{H})\text{Ph}$ groups, bringing extended π -

Table 3. Experimental UV/vis Absorption Bands of Molecule **5k** and TD-DFT Calculated Excitation Energies (nm), Oscillator Strengths (f), and Assignments of the Electronic Transitions (N) of Molecule **1k**^a

N	energy/f	assignment	λ_{abs}
1	431/0.103	122 \rightarrow 123 (95.1%)	427
2	384/0.186	121 \rightarrow 123 (95.7%)	368
3	343/0.087	120 \rightarrow 123 (95.1%)	341
4	328/0.030	119 \rightarrow 123 (88.8%)	
5	300/0.186	122 \rightarrow 124 (87.4%)	292
6	295/0.011	122 \rightarrow 125 (83.9%)	
7	289/0.015	118 \rightarrow 123 (46.8%)	
		122 \rightarrow 126 (25.6%)	
		117 \rightarrow 126 (14.4%)	
8	284/0.013	117 \rightarrow 123 (65.9%)	
		118 \rightarrow 123 (18.4%)	
9	279/0.095	122 \rightarrow 126 (58.6%)	
		118 \rightarrow 123 (23.1%)	
10	273/0.028	122 \rightarrow 127 (35.4%)	
		121 \rightarrow 124 (16.5%)	
		115 \rightarrow 123 (12.9%)	
		114 \rightarrow 123 (11.7%)	
11	271/0.007	116 \rightarrow 123 (65.4%)	
		121 \rightarrow 125 (10.4%)	
12	269/0.096	121 \rightarrow 124 (70.6%)	
13	265/0.026	114 \rightarrow 123 (60.1%)	
		121 \rightarrow 125 (16.8%)	
14	263/0.136	121 \rightarrow 125 (42.2%)	
		115 \rightarrow 123 (27.0%)	
15	262/0.041	122 \rightarrow 127 (44.5%)	
		115 \rightarrow 123 (44.0%)	
16	256/0.162	122 \rightarrow 128 (80.6%)	238
17	255/0.026	121 \rightarrow 126 (75.5%)	
18	250/0.001	122 \rightarrow 129 (62.7%)	
		121 \rightarrow 127 (10.5%)	
19	246/0.006	121 \rightarrow 127 (61.5%)	
		122 \rightarrow 129 (13.6%)	
20	243/0.083	120 \rightarrow 124 (78.9%)	

^aOnly single excitation contributions of more than 10% are given.

delocalization into the systems, leads to a lower optical gap and absorptions in the visible region of the spectra as a result. The calculated absorptions in the range of 350–500 nm imply that the corresponding compounds could produce emission at still higher wavelengths, which would make them candidates for new materials.

CONCLUSIONS

Twenty 1,2-diphospholes have been investigated for the first time within the framework of (time-dependent) density functional theory ([TD]-DFT) and experimentally by UV/vis spectroscopy. It is shown that the PBE0 hybrid density functional combined with the moderate-size def-TZVP AO basis set can be used for the calculation of UV/vis absorption spectra of the title compounds yielding overall excellent agreement between theory and experiment. The simulations allowed a detailed interpretation of the experimental spectra of the title compounds and revealed relationships between chemical modification of the 1,2-diphospholes and their light-absorption properties. In particular, it is shown that variation of substituent at phosphorus atom P1 does not change a HOMO–LUMO gap significantly while the studied 1,2-

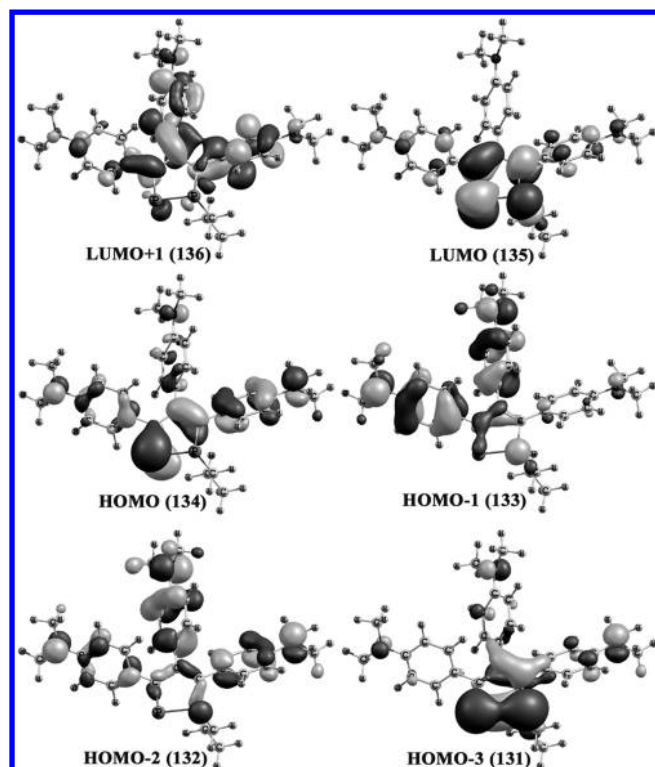


Figure 8. Some frontier molecular orbitals of **1i** (the number of the orbital is shown in the parentheses).

diphospholes are more sensitive to para-substitution in phenyl moieties, which essentially changes the gaps between frontier molecular orbitals. Introduction of electron-donor substituents, containing heteroatoms with lone pairs able to be in conjugation with the phenyl groups, not only shift frontier molecular orbitals but also change their compositions. In particular, *para*-OMe, *para*-NMe₂, and *para*-N(H)Ph derivatives are found to have the smallest HOMO–LUMO gap among all studied molecules. They should absorb in the visible and near UV range and, thus, can be recommended for further practical testing as novel compounds for application in electronic devices.

■ ASSOCIATED CONTENT

📄 Supporting Information

Figure S1. Experimental and simulated UV/vis absorption spectra of **1a** for different basis sets (with the PBE0 functional). Figure S2. Simulated absorption spectra of **3a** for different conformations of the P1-ethyl-substituent. Figure S3. Experimental and simulated absorption spectra of **1b**. Figure S4. Experimental and simulated absorption spectra of **1c**. Table S1. TD-DFT calculated excitation energies, oscillator strengths, and assignments of the electronic transitions of molecule **1g**. Table S2. TD-DFT calculated excitation energies, oscillator strengths, and assignments of the electronic transitions of molecule **1h**. This material is available free of charge via the Internet at <http://pubs.acs.org>.

■ AUTHOR INFORMATION

Corresponding Author

*E-mail: zvereva.elena@gmail.com.

Notes

The authors declare no competing financial interest.

■ ACKNOWLEDGMENTS

A joint scholarship program of the German Service of Academic Exchange (DAAD) and the government of Republic of Tatarstan “Yevgeny Zavoisky” is gratefully acknowledged (EEZ).

■ REFERENCES

- (1) Baumgartner, T.; Reau, R. Organophosphorus π -Conjugated Materials. *Chem. Rev.* **2006**, *106*, 4681–4727.
- (2) Hissler, M.; Lescop, C.; Reau, R. Organophosphorus π -Conjugated Materials: the Rise of a New Field. *J. Organomet. Chem.* **2005**, *690*, 2482–2487.
- (3) Hissler, M.; Dyer, P. W.; Reau, R. The Rise of Organophosphorus Derivatives in π -Conjugated Materials Chemistry. *Top. Curr. Chem.* **2005**, *250*, 127–163.
- (4) Saito, A.; Miyajima, T.; Nakashima, M.; Fukushima, T.; Kaji, H.; Matano, Y.; Imahori, H. Acenaphtho[1, 2-*c*]Phosphole P-Oxide: a Phosphole–Naphthalene π -Conjugated System with High Electron Mobility. *Chem.—Eur. J.* **2009**, *15*, 10000–10004.
- (5) Joly, D.; Tondelier, D.; Deborde, V.; Geffroy, B.; Hissler, M.; Reau, R. Phosphole-Based π -Conjugated Electroluminescent Materials for OLEDs. *New. J. Chem.* **2010**, *34*, 1603–1611.
- (6) Mathey, F. The Organic Chemistry of Phospholes. *Chem. Rev.* **1988**, *88*, 429–453.
- (7) Schäfer, W.; Schweig, A.; Mathey, F. Theory and Application of Photoelectron Spectroscopy. 60. Phospholes. *Electron. Struct. J. Am. Chem. Soc.* **1976**, *98*, 407–414.
- (8) Fadhel, O.; Szieberth, D.; Deborde, V.; Lescop, C.; Nyulaszi, L.; Hissler, M.; Reau, R. Synthesis, Electronic Properties, and Reactivity of Phospholes and 1,1'-Biphospholes Bearing 2- or 3-Thienyl C-Substituents. *Chem.—Eur. J.* **2009**, *15*, 4914–4924.
- (9) Hay, C.; Hissler, M.; Fischmeister, C.; Rault-Berthelot, J.; Toupet, L.; Nyulaszi, L.; Réau, R. Phosphole-Containing π -Conjugated Systems: from Model Molecules to Polymer Films on Electrodes. *Chem.—Eur. J.* **2001**, *7*, 4222–4236.
- (10) Crassous, J.; Reau, R. π -Conjugated Phosphole Derivatives: Synthesis, Optoelectronic Functions and Coordination Chemistry. *Dalton Trans.* **2008**, *48*, 6865–6876.
- (11) Wang, L.; Wang, H. J.; Dong, W. B.; Ge, Q.Y.; Lin, L. Using Three Major Criteria to Evaluate Aromaticity of Five-Member C-Containing Rings and Their Si-, N-, and P-Substituted Aromatic Heterocyclics. *Struct. Chem.* **2007**, *18*, 25–31.
- (12) Cyranski, M. K.; Krygowski, T. M.; Katritzky, A. R.; Schleyer, P. To What Extent Can Aromaticity Be Defined Uniquely? *J. Org. Chem.* **2002**, *67*, 1333–1338.
- (13) Josa, D.; Pena-Gallego, A.; Rodriguez-Otero, J.; Cabaleiro-Lago, E. M. A MP2 and DFT Study of the Aromatic Character of Polyphosphaphospholes. Is the Pyramidalty the Only Factor to Take into Consideration? *J. Mol. Model.* **2011**, *17*, 1267–1272.
- (14) TURBOMOLE V6.4 2012, a program package developed at the University of Karlsruhe and at the Forschungszentrum Karlsruhe GmbH from 1989 – 2007, and at TURBOMOLE GmbH since 2007; available from <http://www.turbomole.com>.
- (15) Bauernschmitt, R.; Haeser, M.; Treutler, O.; Ahlrichs, R. Calculation of Excitation Energies Within Time-Dependent Density Functional Theory Using Auxiliary Basis Set Expansions. *Chem. Phys. Lett.* **1997**, *264*, 573–578.
- (16) Bauernschmitt, R.; Ahlrichs, R. Treatment of Electronic Excitations Within the Adiabatic Approximation of Time Dependent Density Functional Theory. *Chem. Phys. Lett.* **1996**, *256*, 454–464.
- (17) Bauernschmitt, R.; Ahlrichs, R. Stability Analysis for Solutions of the Closed Shell Kohn–Sham Equation. *J. Chem. Phys.* **1996**, *104*, 9047.
- (18) Wang, J.; Wolf, R. M.; Caldwell, J. W.; Kollman, P. A.; Case, D. A. Development and Testing of a General Amber Force Field. *J. Comput. Chem.* **2004**, *25*, 1157–1174.
- (19) Weigend, F.; Ahlrichs, R. Balanced Basis Sets of Split Valence, Triple Zeta Valence and Quadruple Zeta Valence Quality for H to Rn:

Design and Assessment of Accuracy. *Phys. Chem. Chem. Phys.* **2005**, *7*, 3297–3305.

(20) Eichkorn, K.; Treutler, O.; Öhm, H.; Häser, M.; Ahlrichs, R. Auxiliary Basis Sets to Approximate Coulomb Potentials (Chem. Phys. Letters 240 (1995) 283–290). *Chem. Phys. Lett.* **1995**, *242*, 652–660.

(21) Eichkorn, K.; Weigend, F.; Treutler, O.; Ahlrichs, R. Auxiliary Basis Sets for Main Row Atoms and Transition Metals and Their Use to Approximate Coulomb Potentials. *Theor. Chem. Acc.* **1997**, *97*, 119–124.

(22) Weigend, F.; Häser, M.; Patzelt, H.; Ahlrichs, R. RI-MP2: Optimized Auxiliary Basis Sets and Demonstration of Efficiency. *Chem. Phys. Lett.* **1998**, *294*, 143–152.

(23) Perdew, J. P.; Burke, K.; Ernzerhof, M. Generalized Gradient Approximation Made Simple. *Phys. Rev. Lett.* **1996**, *77*, 3865–3868.

(24) Perdew, J. P.; Burke, K.; Ernzerhof, M. Generalized Gradient Approximation Made Simple [Phys. Rev. Lett. *77*, 3865 (1996)]. *Phys. Rev. Lett.* **1997**, *78*, 1396–1396.

(25) Gross, E. U. K.; Dobson, J. F.; Petersilka, M. Density Functional Theory II, Springer Series in *Topics in Current Chemistry*; Nalewajski, R. F., Ed.; Springer: Heidelberg, Germany, 1996.

(26) Casida, M. E. *Recent Advances in Density Functional Methods*; Chong, D. P., Ed.; World Scientific: Singapore, 1995; Vol. 1.

(27) Furche, F. On the Density Matrix Based Approach to Time-Dependent Density Functional Response Theory. *J. Chem. Phys.* **2001**, *114*, 5982.

(28) *Reviews in Computational Chemistry*; Lipkowitz, K.B., Larter, R., Cundari, T. R., Eds.; John Wiley & Sons, Inc.: Hoboken, NJ, 2004; Vol. 20.

(29) Solomon, R. V.; Bella, A. P.; Vedha, S. A.; Venuvanalingam, P. Designing Benzosiloles for Better Optoelectronic Properties Using DFT & TDDFT Approaches. *Phys. Chem. Chem. Phys.* **2012**, *14*, 14229–14237.

(30) Dierksen, M.; Grimme, S. The Vibronic Structure of Electronic Absorption Spectra of Large Molecules: A Time-Dependent Density Functional Study on the Influence of “Exact” Hartree–Fock Exchange. *J. Phys. Chem. A* **2004**, *108*, 10225–10237.

(31) Peach, M. J. G.; Le Sueur, C. R.; Ruud, K.; Guillaume, M.; Tozer, D. J. TDDFT Diagnostic Testing and Functional Assessment for Triazene Chromophores. *Phys. Chem. Chem. Phys.* **2009**, *11*, 4465–4470.

(32) Aittala, P. J.; Cramariuc, O.; Hukka, T. I.; Vasilescu, M.; Bandula, R.; Lemmetyinen, H. A TDDFT Study of the Fluorescence Properties of Three Alkoxyphenylindolizine Derivatives. *J. Phys. Chem. A* **2010**, *114*, 7094–7101.

(33) Petsalakis, I.; Georgiadou, D.; Vasilopoulou, M.; Pistolis, G.; Dimotikali, D.; Argitis, P.; Theodorakopoulos, G. Theoretical Investigation on the Effect of Protonation on the Absorption and Emission Spectra of Two Amine-Group-Bearing, Red “Push–Pull” Emitters, 4-Dimethylamino-4'-nitrostilbene and 4-(dicyanomethylene)-2-methyl-6-p-(dimethylamino) styryl-4H-pyran, by DFT and TDDFT Calculations. *J. Phys. Chem. A* **2010**, *114*, 5580–5587.

(34) Adamo, C.; Barone, V. Toward Reliable Density Functional Methods Without Adjustable Parameters: The PBE0 model. *J. Chem. Phys.* **1999**, *110*, 6158.

(35) Rienstra-Kiracofe, J. C.; Tschumper, G. S.; Schaefer, H. F., III; Sreela, N.; Ellison, G. B. Atomic and Molecular Electron Affinities: Photoelectron Experiments and Theoretical Computations. *Chem. Rev.* **2002**, *102*, 231–282.

(36) Becke, A. D. A New Mixing of Hartree–Fock and Local Density Functional Theories. *J. Chem. Phys.* **1993**, *98*, 1372.

(37) Frisch, M. J.; et al. *Gaussian 03*, revision B.05; Gaussian, Inc.: Wallingford, CT, 2004. E.E.Z. is indebted to all staff-members of the Supercomputer centre of the Kazan Scientific Centre of the Russian Academy of Sciences and especially to Dr. D. Chachkov for technical assistance in these computations.

(38) <http://www.chemcraftprog.com>.

(39) Grace, (c) 1996–2008 Grace Development Team, see <http://plasmagate.weizmann.ac.il/Grace>.

(40) Milyukov, V. A.; Bezkishko, I. A.; Zagidullin, A. A.; Sinyashin, O. G.; Hey-Hawkins, E. Reactions of Sodium 3,4,5-Triphenyl-1,2-Diphosphacyclopentadienide With Alkyl Halides and Silicon and Tin Chlorides. *Russ. Chem. Bull.* **2010**, *59*, 1232–1236.

(41) Matano, Y.; Fujita, M.; Saito, A.; Imahori, H. Synthesis, Structures, Optical and Electrochemical Properties, and Complexation of 2,5-Bis(Pyrrol-2-yl)Phospholes. *C. R. Chim.* **2010**, *13*, 1035–1047.

(42) Oziminski, W. P.; Dobrowolski, J.Cz. On the Tautomerism, Planarity, and Vibrations of Phospholes. *Chem. Phys.* **2005**, *313*, 123–132.

(43) Friedel, R. A.; Orchin, M. *Ultraviolet Spectra of Aromatic Compounds*; Wiley: New York, 1951.

(44) Hirayama, K. *Handbook of UV & visible absorption spectra of organic compounds*; Plenum Press: New York, 1967.

(45) Raciszewski, Z.; Braye, E. H. Fluorescence of Phenyl-Substituted Heterocyclopentadienes: Comparison of the Effects of N, P, As, P→O and of the Number of Phenyl Substituents. *Photochem. Photobiol.* **1970**, *12*, 429–432.

(46) Zhang, Y.; Yang, W. A Challenge for Density Functionals: Self-Interaction Error Increases for Systems With a Noninteger Number of Electrons. *J. Chem. Phys.* **1998**, *109*, 2604–2608.

(47) Gritsenko, O.; Ensing, B.; Schipper, P. R. T.; Baerends, E. J. Comparison of the Accurate Kohn–Sham Solution with the Generalized Gradient Approximations (GGAs) for the S_N2 Reaction F[−] + CH₃F → FCH₃ + F[−]: a Qualitative Rule to Predict Success or Failure of GGAs. *J. Phys. Chem. A* **2000**, *104*, 8558–8565.

(48) Kronik, L.; Stein, T.; Refaely-Abramson, S.; Baer, R. Excitation Gaps of Finite-Sized Systems from Optimally Tuned Range-Separated Hybrid Functionals. *J. Chem. Theory Comput.* **2012**, *8*, 1515–1531.

(49) Graule, S.; Rudolph, M.; Shen, W.; Gareth Williams, J. A.; Lescop, C.; Autschbach, J.; Crassous, J.; Reau, R. Assembly of π -Conjugated Phosphole Azahelicene Derivatives into Chiral Coordination Complexes: an Experimental and Theoretical Study. *Chem.—Eur. J.* **2010**, *16*, 5976–6005.

(50) Shorygin, P. P. Raman Scattering and Conjugation. *Russ. Chem. Rev.* **1971**, *40*, 367–392.

(51) El-Nahas, A. M.; Mangood, A. H.; El-Shazly, T. S. Theoretical Investigation of the Conducting Properties of Substituted Phosphole Oligomers. *Comput. Theor. Chem.* **2012**, *980*, 68–72.